*International Journal of Remote Sensing*, 2015
Vol. 36, No. 11, 2920–2933, http://dx.doi.org/10.1080/01431161.2015.1051632





# Validation of ground-based microwave radiometer data and its application in verifying atmospheric stability over Mahbubnagar during 2011 monsoon and post-monsoon seasons

P.P. Leena*, K.K. Dani, Asha Nath, S.D. Sanap, G. Pandithurai, and V. Anil Kumar

*Indian Institute of Tropical Meteorology, Pashan, Pune 411008, India*

(*Received 12 December 2014; accepted 30 March 2015*)

Atmospheric instabilities, mainly convection, depend on temperature distribution and moisture availability. The development of convection can often lead to the formation of clouds and precipitation, release of latent heat, etc. The initiation or development of instabilities has to be studied in detail with high-resolution, ground-based instruments such as ground-based microwave radiometric measurements. In this study we evaluated ground-based microwave radiometer data (MWR)-retrieved temperature and relative humidity profiles and compared these to radiosonde observations. Analysis showed that MWR-measured temperature (specific humidity) has a warm (wet) bias below 3 km and cold (dry) bias above that altitude. Correlation of stability indices estimated from radiometer and radiosonde showed fairly good correlation, with a correlation coefficient greater than 0.5 with 95% significance. MWR was then utilized for the verification of atmospheric stability over Mahbubnagar (16° 44′ N, 77° 59′ E), India, during the second half of the monsoon and start of post-monsoon seasons. Radiometric observations showed strong day-to-day variation of atmospheric parameters as well as thermodynamic indices during the monsoon, which were weak during the post-monsoon season. The seasonal mean of thermodynamic indices and the associated seasonal difference showed that thunderstorm potential is higher during the post-monsoon season over the study site.

## 1. Introduction

Temperature and water vapour play an important role in the atmosphere. The distribution of water vapour influences various atmospheric processes such as deep convection, precipitation, radiation transfer, and energy balance. Atmospheric instability/processes, mainly development of convection, can often lead to formation of clouds and precipitation, release of latent heat, etc. Several studies have reported on the seasonal and long-term variation in various atmospheric parameters such as outgoing longwave radiation (OLR), sea surface temperature (SST), precipitable water, and clouds, which have effects on convective activity over different regions (Dai 2001; Gettelman et al. 2002; Ueno and Aryal 2008; Sapra et al. 2011; Venkat Ratnam et al. 2013). Few studies have investigated the diurnal variation in convection. In general, understanding atmospheric stability over the tropics is a complex issue, but can be overcome to a certain extent by estimating stability indices as well as through continuous monitoring of the atmosphere. In other words, stability indices are essential for understanding the thermodynamic structure of the atmosphere, especially in troposphere, which needs to be estimated from observations. We

*Corresponding author. Email: leena@tropmet.res.in

know that the estimation of stability indices derived from thermodynamical parameters requires highly accurate data sets of temperature and water vapour.

Earlier studies using radiosondes have shown that they are suitable for measuring vertical profiles of atmospheric parameters such as temperature ($T$), relative humidity (RH), and pressure (Elliott and Gaffen 1991; Gettelman et al. 2006; Sun et al. 2010; Kwon et al. 2012). However, there are limitations for example radiosonde measurements/ data are available at most only twice per day, which is not sufficient to capture the thermodynamic state of the atmosphere. Apart from this, it is also seen that radiosonde measurements are not satisfactory, especially during low-humidity conditions or when there are large horizontal or temporal gradients in humidity structure (Han et al. 1994), as these have poor temporal resolution. Recent studies have shown that ground-based microwave radiometer data (MWR), is an alternative source or is suitable for the study of thermodynamical state of atmosphere and its temporal evolution (Ware et al. 2003; Cimini et al. 2006; Löhnert and Maier 2012; Madhulatha et al. 2013 and references there within). All the above-mentioned studies have shown that MWR has the advantage of continuous monitoring of the atmosphere up to a maximum altitude of 10 km with a time interval of about 2 min. More details about MWR and its data retrieval are explained in the following section. Apart from demonstrating the robustness of MWR, many studies (e.g. Chan 2009; Chan and Hon 2011; Cimini et al. 2011) have shown that data from this instrument can be used in nowcasting of convective weather. Although the above-mentioned studies discuss the advantages of MWR data, some have observed/ reported bias in temperature and RH measurements. A recent study by Sanchez et al. (2012) reported a bias in temperature and humidity measurements obtained by MWR. These authors applied bias correction using a linear adjustment method, which significantly improved vertical temperature and water vapour density profile accuracy. That study, along with some others from the Indian region (Madhulatha et al. 2013; Venkat Ratnam et al. 2013), have also shown bias in radiometer retrieved temperature and humidity profiles.

Considering these features of MWR, as a first step in the present study we validated the MWR observations with radiosonde observations by comparing the temperature and humidity profiles from each. For a detailed comparison we correlated several other atmospheric parameters and stability indices derived from MWR with parameters estimated from radiosonde measurements. Finally, considering the advantages of MWR, we utilized it to verify atmospheric stability during the monsoon and post-monsoon seasons over Mahbubnagar, a site within a rain shadow region. This work will be useful to chart the evolution of the thermodynamic state of the atmosphere over a rain shadow region, as well as to verify the robustness of microwave radiometric observations.

## 2. Instruments used

The Integrated Ground Observational Campaign during the Cloud Aerosol Interaction and Precipitation Enhancement Experiment (CAIPEEX-IGOC) campaign was conducted by the Indian Institute of Tropical Meteorology (IITM) from 21 June to 11 November 2011 over the Indian southern peninsular region at Mahbubnagar (16° 44′ N, 77° 59′ E). The observational site is a semi-urban region located on the edge of the Deccan Plateau 440 m above mean sea level (AMSL). It is to be noted that the study location is subject to both SW and NE monsoons; during the study period the region received part of the former. Along with a host of other instruments, a microwave radiometer was operated continuously during the entire period of the campaign. This provides vertical profiles of temperature, water vapour, and liquid water. The radiosonde was launched once per day around noon local time (about 06.00 GMT). A detailed description of the instrument and data used are presented below.

### 2.1. *Microwave radiometer*

The ground-based microwave radiometer used in the CAIPEEX IGOC campaign was a MP-3000A (Radiometrics Corp., USA), a 35-channel temperature, water vapour, and liquid water profiler. The MP-3000A incorporates two radiofrequency (RF) subsystems in the same cabinet, which share the same antenna and antenna pointing system. Temperature profiles are obtained by measuring the radiation intensity or brightness temperature at points along the side of the oxygen absorption band at 60 GHz. Similarly, water vapour profiles can be obtained by observing the intensity and shape of emission from pressure-broadened water vapour lines. The line near 22 GHz is suitable for ground-based profiling in relatively moist areas. Several retrieval techniques are currently available but traditionally, microwave radiometer retrieval uses non-linear (e.g. iterative), linear (e.g. regression), or neural network (NN) methods, partially overcoming the lack of sensitivity at higher levels by incorporating statistical correlations between lower and higher levels (Cimini et al. 2011). With the microwave radiometer used in this study, the brightness temperature algorithm for level 1 products is a four-point non-linear model whereas retrieval algorithms for level 2 products are NNs. Neural networks supplied by Radiometrics Corp. are derived using the history of radiosonde profiles (more details can be obtained from the Radiometrics profiler operator's manual, http://radiometrics.com or http://doi.org/10.12898/ES0702FR). For the present study region, a NN trained on radiosonde data from the University of Wyoming for the station Hyderabad (located about 102 km from campaign region) is used. This retrieves temperature and RH profiles with a temporal resolution of 2 min and with height resolution as follows: up to 500 m with 50 m, 500 m–2 km with 100 m, and 2–10 km with 250 m. For the present study, the entire data set was interpolated to height intervals of 100 m resolution and the hourly average recorded. Apart from obtaining vertical profiles, the radiometer also provides surface parameters (i.e. temperature, pressure, and RH) and integrated products such as vapour, liquid, and cloud base height.

It is to be noted that radiometer retrieval accuracy depends on calibration, and thus it is important to describe the quality and timeliness of liquid nitrogen ($LN_2$) calibration. The instrument was calibrated on 24 June 2011 and this procedure typically takes 1–2 hours, after which the regular observation cycle is resumed. The manufacturer supplied a calibration target, which comprises a box of expanded polystyrene foam containing a permeable microwave absorber. This is filled with $LN_2$ and placed on top of the radiometer, and it views emissions from the absorber through the base of the polystyrene box, which has low loss at microwave frequencies. This provides a black body at low temperature that can be accurately calculated. The contrast between radiometer measurements when viewing this and the internal black body near ambient temperatures is used to derive values of the brightness temperature of the noise diode (ND) (Hewison and Gaffard 2003). The time series of the ND for different frequencies is shown in Figure 1, and was found to be stable during calibration. The average value of the ND is then used for the entire campaign.

### 2.2. *Radiosonde*

GPS radiosonde balloon flights were carried out to probe the atmosphere vertically up to a maximum of 30 km, with good spatial resolution. This instrument uses sensors to measure

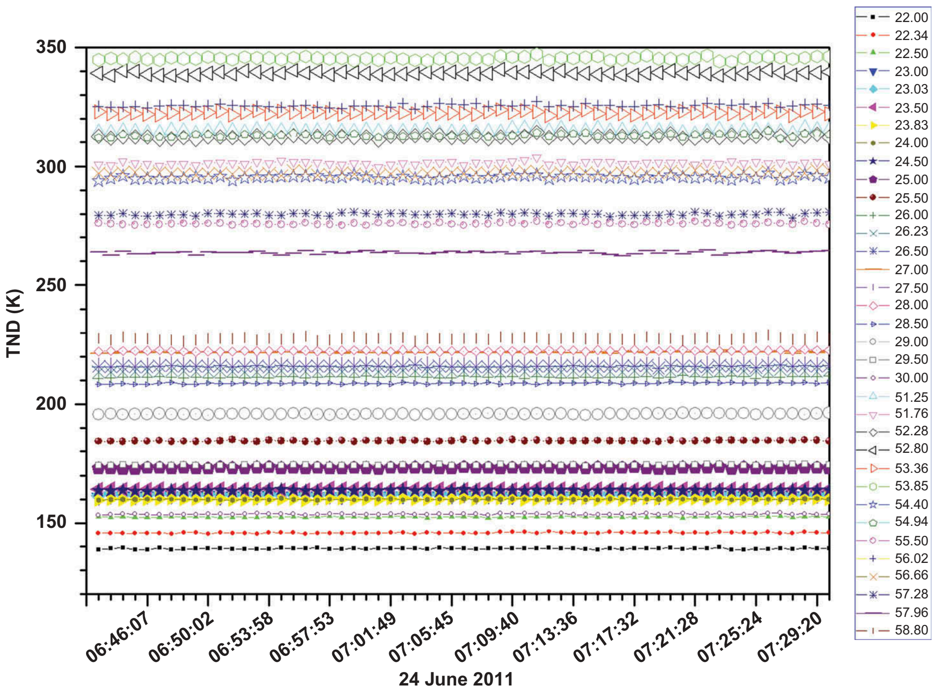


Figure 1. Plot showing the time series of TND for different frequencies (GHz) obtained from $LN_2$ calibration on 24 June 2011.

atmospheric parameters such as temperature, pressure, and RH, and the GPS incorporated helps in deriving horizontal wind speed and direction. In the present campaign, balloon flights were carried out using Vaisala RS92-SGP sensors. This is the DigiCORA® Sounding System MW31 with DigiCORA® sounding software (The Vaisala DigiCORA® Sounding System MW31 is a sounding receiving station for meteorological and defence applications). These sensors operate on the 400 MHz meteorological band with code-correlating GPS wind finding (further details at www.vaisala.com). As a part of this campaign, the radiosonde was launched daily from 2 August to 10 November 2011 at the observation site around noon, local time (about 06.00 GMT).

The data obtained from both instruments were interpolated to height intervals of 100 m resolution. Thus we used 100 m interpolated temperature and RH data for the present study.

## 3. Validation of MWR with GPS radiosonde

Three months' (August–October 2011) data from radiosonde and radiometer were used for the comparison of $T$ and specific humidity (SH). Figure 2($a$) shows a typical comparison of $T$ and SH for 31 August 2011. The temperature profiles (Figure 2($a$)) from both instruments and the trends match well. The difference between the instruments was estimated by using radiosonde (RS) as the reference, and it is observed that this varies between −2 K and 3 K for a single day. To determine the variation in humidity with respect to altitude in the troposphere, we derived SH using temperature, pressure, and RH separately for both instruments using the method of Ross and Elliott (1996), and a typical example is presented in Figure 2

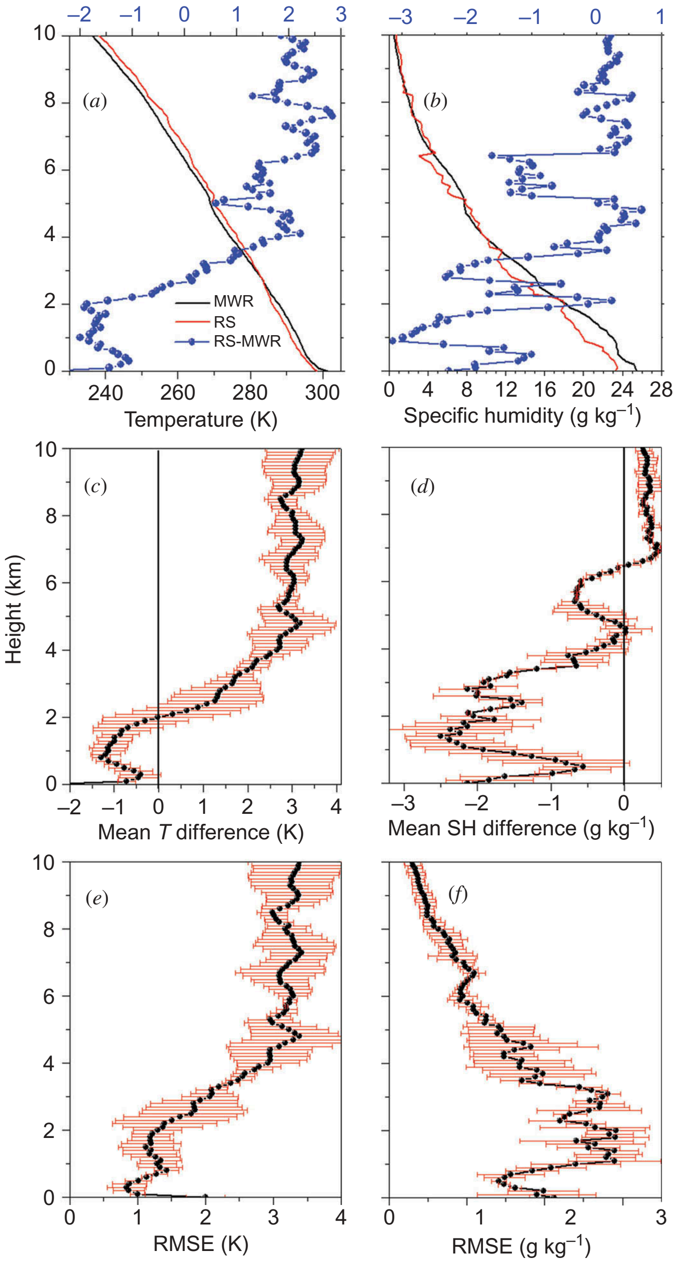


Figure 2. Plot showing the comparison for a typical day (31 August 2011) (*a*, *b*), three-month mean difference along with standard deviation (*c*, *d*), and three-month mean RMSE along with standard deviation (*e*, *f*).

(*b*). It is observed that SH profiles from both instruments match well with a variation of −3.2 to 0.5 g kg$^{-1}$. This variation in SH is consistent with previously reported values over the tropics (Kishore et al. 2011). The difference (radiosonde minus radiometry) is also comparable to previously reported results (e.g. Venkat Ratnam et al. 2013) over the Indian region.

As part of the detailed quantitative analysis, we calculated the monthly bias (data not shown) as well as root mean square error (RMSE), along with mean bias or difference and RMSE for *T* and SH (Figures 2(*c*)–(*f*)). From Figure 2(*c*), a temperature bias of −1 to 3 K, excluding the error, can be observed in MWR with a warm bias of about 2 K below 3 km and a cold bias of 3 K above 3 km. From Figure 2(*d*), the mean difference in SH varies between −2.5 and 0.5 g $kg^{-1}$ with a wet bias below 3 km and dry bias above that altitude. The maximum wet and dry bias observed is about −2 and about 0.5 g $kg^{-1}$, respectively. The mean difference with respect to altitude showed different behaviour above and below 6 km: above 6 km the profiles are very close, with a negligible dry bias.

RMSE illustrates that the error in retrieved temperature (Figure 2(*e*)) increases with altitude whereas that in SH decreases with altitude (Figure 2(*f*)). Below 4 km the mean RMSE showed a maximum of 2 K in temperature, suggesting that retrievals are almost similar to radiosonde measurements in the lower troposphere. In case of SH, it showed better matching above 4 km, possibly due to the exponential decay of SH with altitude. Hence, from the overall analysis it is clear that MWR retrieval matches well with radiosonde, especially in the lower troposphere. This suggests that MWR can be used for meteorological applications. We have seen the comparison between temperature and SH in this section but we know that *T* and SH values alone are not sufficient to describe the stability of the atmosphere quantitatively. In order to verify this, we need several other atmospheric parameters and thermodynamic indices. For detailed comparison, different thermodynamic indices were derived from MWR and GPS radiosonde observations and we examined their correlation. Various atmospheric parameters such as cloud base height (CBH), dew point temperature ($T_d$) at 850 hpa, and seven other thermodynamic indices were calculated. Different thermodynamic indices (along with abbreviations) and their correlation (*r*) are given in Table 1, and Figure 3 shows the correlation plots of these indices.

All the above-mentioned parameters are well correlated except for lapse rate (LR) upto 500 from 700 hpa and lifted index (LI). In general, most of the variables showed correlation coefficient above 0.5. The correlation coefficient of thermodynamic indices (see Table 1) obtained from this analysis matches with that reported by Madhulatha et al. (2013) for another Indian tropical station, Gadanki. Indices such as total total index (TTI) and *K*-index (KI) showed correlation similar to that reported by Chan and Hon (2011). It is to be noted that CBH obtained from radiometeric observation was correlated with the lifting condensation level (LCL) of radiosonde for which the highest correlation was observed. The non-zero intercept for all correlated parameters suggests that there is a bias which may be due to that in for either *T* or RH. It is also observed that the slope obtained from each correlation analysis is not 1, which suggests that there is a bias in temperature and humidity with respect to altitude, which is clear from the previous section. However, the overall analysis suggests that the quality of MWR profiles is sufficient to calculate thermodynamic indices, which help in explaining the stability of the troposphere. Therefore, for further analysis, we used MWR data to verify atmospheric stability during the monsoon and post-monsoon seasons.

## 4. Results and discussion

### *4.1. Day-to-day variation in atmospheric parameters and thermodynamic indices*

In order to study the atmospheric stability during the monsoon (August–September) and post-monsoon (October–November) seasons we first examined the variation in atmospheric parameters obtained from the radiometer, some being direct measurements and

Table 1. List of thermodynamic indices used in the study and their correlation ($r$) values between GPS and MWR.

| S. No | Thermodynamic indices | $r$ |
|---|---|---|
| 1 | Lapse rate (LR) 700–500 hpa [K km$^{-1}$]<br>Helps in explaining the instability present in the atmosphere (Madhulatha et al. 2013) | −0.11 |
| **2** | Lifted index (LI) [°C]<br>Mainly considers temperature difference between an air parcel lifted adiabatically ($T_p$) and the temperature of the environment at a given pressure in the troposphere, usually at 500 mbar (Galway 1956), and is given by<br>$T_{p500} - T_{500}$ | 0.31 |
| **3** | Total total index (TTI) [°C]<br>TTI is a commonly used convective index (Miller 1967) and is given by<br>$T_{850} + T_{d850} - 2T_{500}$ | 0.59 |
| **4** | $K$-index (KI) [°C]<br>KI was developed by George (1960) for forecasting air mass thunderstorm) and it is given by,<br>$(T_{850} - T_{500}) + T_{d850} + (T_{700} - T_{d700})$ | 0.61 |
| **5** | Showalter index (SI) [°C]<br>This index mainly considers the difference between the observed temperature at 500 hPa ($T_{500}$) and the temperature of an air parcel after it has been lifted pseudo-adiabatically to 500 from 850 hPa (Showalter 1953) | 0.56 |
| 6 | Convective temperature (Conv temp) [°C]<br>Mainly explains the surface heating effect resulting from the rising of an air parcel with no mechanical lifting<br>(http://www.theweatherprediction.com or Madhulatha et al. 2013) | 0.69 |
| 7 | Convective available potential energy (0–3 km) [J kg$^{-1}$]<br>CAPE is a measure of amount of energy that is available during convection (Venkat Ratnam et al. 2013) and it is a potential indicator of the convective activity in the atmosphere | 0.53 |



some estimated. The temperature and RH were directly measured, whereas dew point temperature and equivalent potential temperature (EPT) were estimated from radiometer data. It should be noted that as a representation of each season we considered three consecutive days in August for the monsoon and also in October for the post-monsoon. In order to demonstrate day-to-day variation along with a seasonal picture, we made recordings on three consecutive days. It should be noted that more than 90% of the days in each month show the same level of diurnal variation with corresponding seasonal/monthly change. The day-to-day variation in all four parameters with respect to altitude is shown Figure 4. From this figure it will be seen that all parameters exhibit a strong day-to-day variation with respect to altitude in the monsoon, but a weak variation during the post-monsoon season. It is observed that in both seasons, temperature (Figure 4(*a*)) exhibits a clear diurnal variation up to a maximum altitude of 2 km with more heating below 1 km altitude. It is also seen that diurnal variation in temperature is weak in higher altitudes. Even radiometric observation showed variation in the convective boundary layer. From the temperature variation it will be seen that heating is well defined in the post-monsoon compared with the monsoon season.

In regard to RH (Figure 4(*b*)) there is marked day-to-day variation with respect to altitude during the monsoon, whereas as it is relatively weak in the post-monsoon season. Below 2 km altitude, RH was at a maximum of 100% very early in the morning

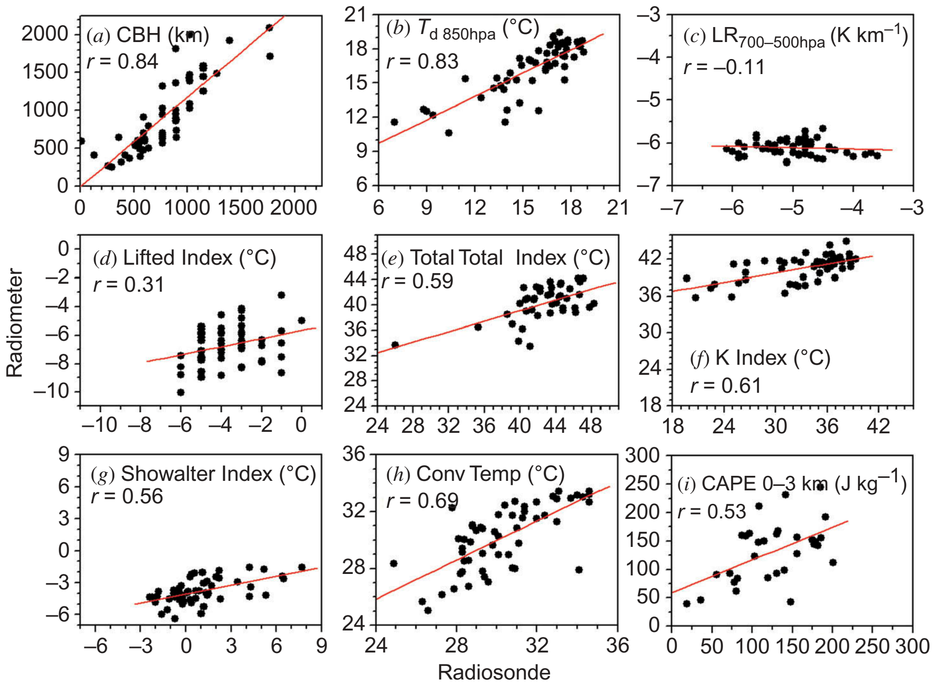


Figure 3. Scatterplot showing atmospheric parameters and thermodynamic indices derived from radiosonde and radiometer observations.

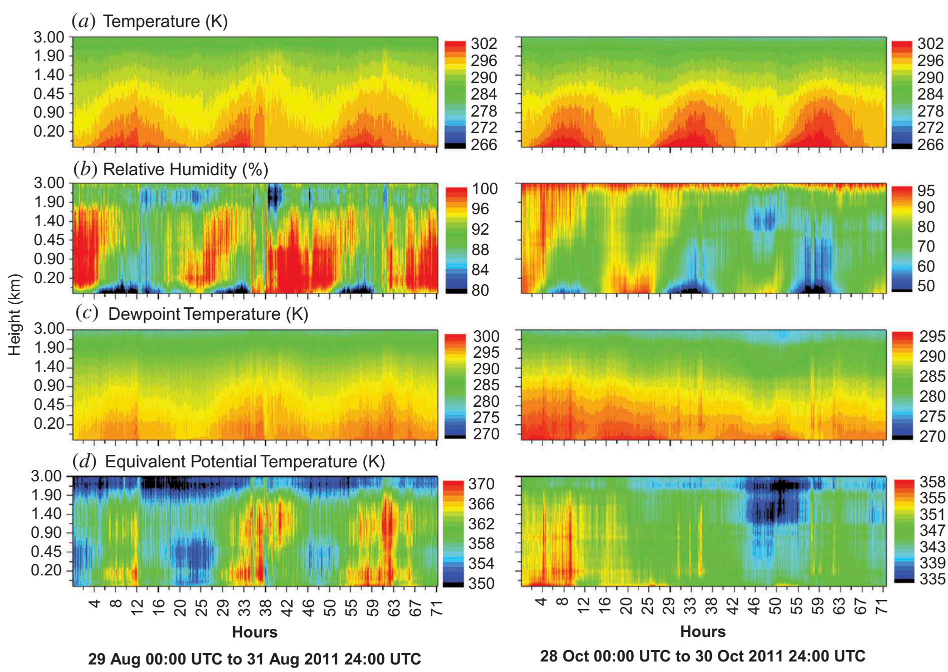


Figure 4. Day-to-day variation in (a) temperature, (b) relative humidity, (c) dew point temperature, and (d) EPT with respect to altitude observed separately using microwave radiometer over 3 consecutive days in August and October 2011.

and late evening during the monsoon season while at noon time it was about 80% in the boundary layer, as expected. As in the case of temperature, RH also showed weak diurnal variation with respect to altitude. It is also observed that RH is comparatively low in the post-monsoon season (50–90%). These variations in $T$ and RH can contribute to instability in the atmosphere, which is clearly seen even from the estimated dew point temperature ($T_d$) and EPT. $T_d$ clearly shows diurnal variation like that of $T$ and RH, with a maximum up to 2 km altitude in the monsoon but it is weak in the post-monsoon season. Up to 1 km altitude $T_d$ was very high, implying the presence of a large quantity of moisture during the monsoon, and the converse in the post-monsoon. This clearly shows the presence of large low level moisture content during the monsoon season. Apart from the variation in $T$, RH, and $T_d$, we also observed variation in the EPT to see the variability of moist static energy of the atmosphere. According to the definition of EPT, under stable conditions EPT increases with altitude and, if it decreases with altitude, convection can occur. The EPT of air parcels at different altitudes provides a measure of instability of the air column. EPT also showed day-to-day variation similar to that of temperature in the monsoon, which is absent during the post-monsoon season. In general, during the monsoon season low EPT is observed early in the morning, increasing as the temperature rises during the day. Variation in EPT with respect to altitude showed that it reached maximum up to 2 km altitude, suggesting an increase in moist static energy. The strong day-to-day variation in atmospheric parameters suggests that the monsoon is well established over the study site and that instability accompanies large-scale convection or moisture transport. In order to investigate thermodynamic structure or instability in the troposphere in detail, we recorded the day-to-day variation in the nine above-mentioned parameters for the monsoon and post-monsoon seasons separately, which is shown in Figures 5 and 6. It should be noted that we present a five-point running mean (i.e. 10-min averaged points) in these figures. Since the data are available for every 2-min interval, we represented them in such a way as to provide a smooth behaviour for the variables.

In general all the atmospheric parameters and thermodynamic indices showed strong day-to-day variation during the monsoon compared with the post-monsoon. As mentioned above, the $T_d$ at 850 hPa is comparatively high in the monsoon compared with the post-monsoon season, confirming the availability of low-level moisture. This will help in the formation of rain-bearing clouds with low CBH over the study region, which can even precipitate. Formation of clouds with lower CBH is clearly seen from the diurnal variation in CBH. During the monsoon season, CBH is confined within or less than 1 km whereas it is twice in post-monsoon season, with strong day-to-day variation in both seasons. The CBH has its maximum around 12.00 GMT and the minimum (<200 m above ground level) in the evening and very early morning. This is consistent with variation in water vapour levels. This variation in low-level moisture and CBH shows that there is a possibility of the development of deep convective or rain-bearing clouds either in the early morning or late evening over the study site during the second half of the monsoon season.

As mentioned above, the variation in thermodynamic indices such as LI, TTI, KI, Showalter index (SI), convective temperature (Conv temp), and convective available potential energy (CAPE) will be also useful to explain the thermodynamic state of the atmosphere during the monsoon and post-monsoon seasons. Considering this, for the present study we estimated seven thermodynamic indices (Table 1) from microwave radiometer observation, and these are shown in Figures 5 and 6. Most of the indices exhibit strong day-to-day variation in the monsoon compared with post-monsoon. In

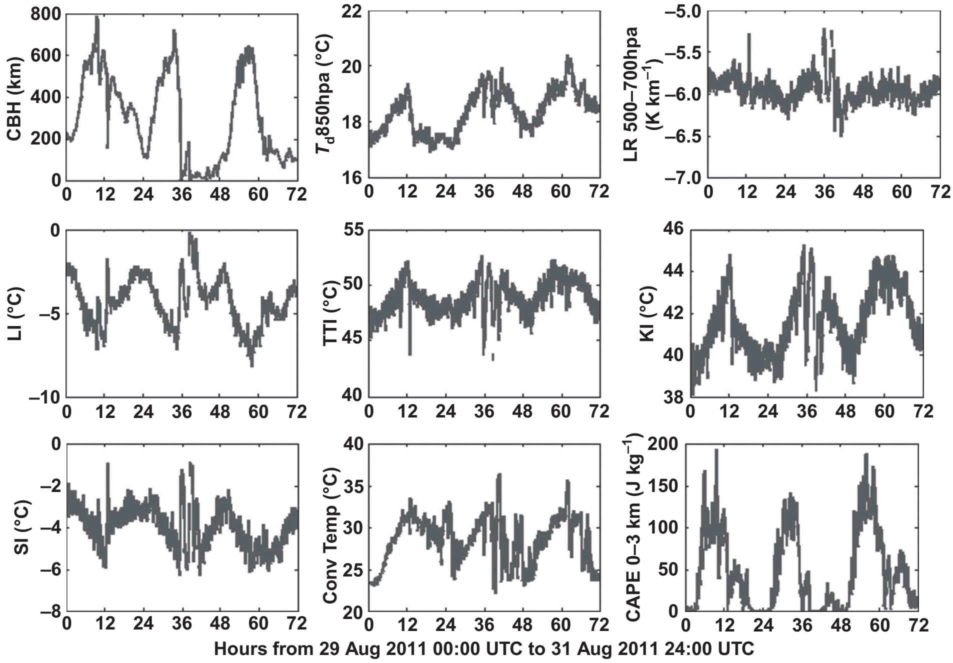


Figure 5. Day-to-day variation (five-point running mean) for CBH, $T_d$ 850 hpa, LR 700–500 hpa, LI, TTI, KI, SI, Conv temp, and CAPE at 0–3 km estimated from microwave radiometric observation for 29–31 August 2011.

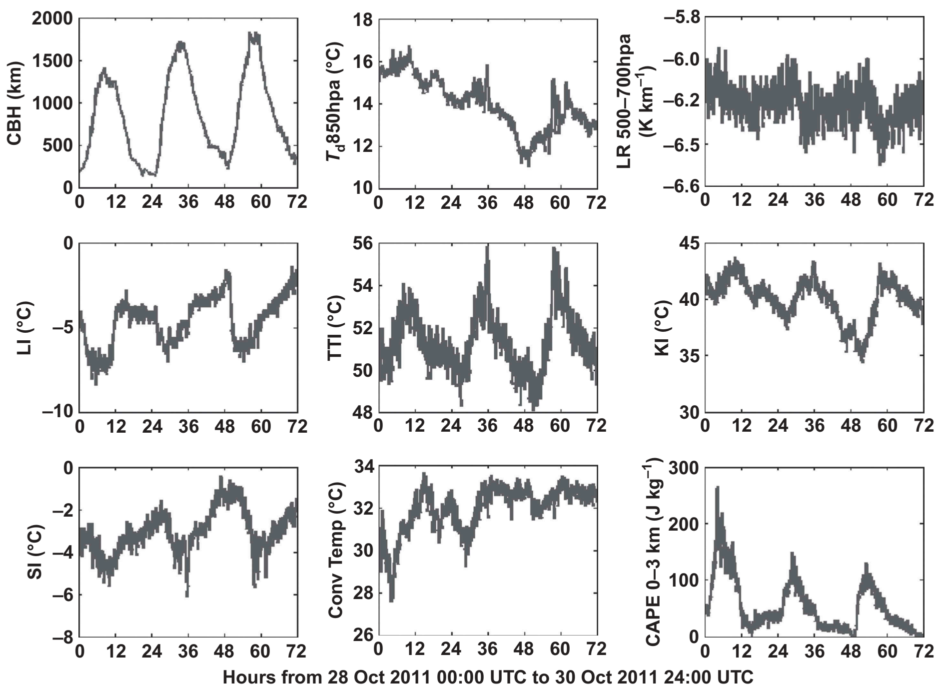


Figure 6. As Figure 5, but for 28–30 October 2011.

general we find a similar diurnal variation in indices in both seasons. Most lR, which indicates the stability/instability of the atmosphere, did not show a clear diurnal cycle or day-to-day variation but negative LR showed that the atmosphere is highly unstable in both seasons. From the variation in LI it is observed that this is negative throughout both day and night, suggesting an unstable atmosphere. In both seasons the values vary within the same range and with similar temporal variation. TTI and KI, which represent the availability of moisture, also exhibited a clear diurnal variation similar to that of $T_d$ (high at noon and low early in morning and in the evening). TTI values exceeded 50 after 04.00 UTC but after 12.00 UTC they decreased; similarly KI was >40 after 04.00 UTC. This variation is consistent with variation in moisture. SI showed a similar diurnal variation to that of LI, with negative values, indicating that the planetary boundary layer is unstable with respect to the middle troposphere. Conv temp did not show significant day-to-day variation in the post-monsoon season but interestingly it is observed that the lower limit is higher in this season compared with the monsoon. It is also seen that it started increasing around 04.00 UTC and followed the same temporal variation as that of temperature in the monsoon. CAPE (0–3 km) also showed a clear diurnal cycle with a maximum between 04.00 and 12.00 UTC, thereafter decreasing in the monsoon. In the boundary layer itself it is observed that CAPE reached a maximum of 200 J $kg^{-1}$ for both seasons, and sometimes 300 J $kg^{-1}$ in the post-monsoon. Our analysis suggests that during the monsoon season as the day progresses the atmosphere becomes more conducive to convection, with all the stability parameters showing instability up to 12.00 UTC; in the evening the atmosphere becomes inhibitive to convection. In the post-monsoon season the stability indices did not show such clear temporal variation as in the monsoon season, which suggests that in post-monsoon season localized convective activity such as thunderstorms will be more likely.

### *4.2. Seasonal variation in thermodynamic indices*

As a quantitative measure of atmospheric instability during both seasons, we observed seasonal variation in six thermodynamic indices along with the difference (August–September minus October–November), which are shown in Figure 7. It should be noted that these six indices are well established in explaining the thermodynamic state of the atmosphere, including the possibility of severe convective events over a single location. In general, from the figure it is noted that all thermodynamic indices show a clear diurnal variation in both seasons, which is similar to previously mentioned results. Although LI showed similar diurnal variation in both seasons, with negative values, it is observed that LI is more likely to be negative in the early morning (before 04.00 GMT) in the post-monsoon season. This is clear from the fact that there is a positive difference (about 2) during that time, suggesting the possibility of thunderstorms. Interestingly, TTI showed a higher seasonal mean during the post-monsoon than the monsoon season, which suggests high moisture availability at both low and higher levels (500 hpa) during the post-monsoon season. KI and SI showed no distinct between-season variation, which is clear from their negligible difference. Conv temp showed higher values during the post-monsoon season than the monsoon. It is well known that Conv temp is the temperature required that the surface of the earth must warm to in order for thunderstorms to occur in the absence of synoptic forcing mechanisms. The difference between the two seasons showed a negative value (about 3°C),suggesting that the thunderstorm potential is higher during the post-monsoon season over the study site. Though CAPE showed no distinct variation between monsoon and post-monsoon, it is interesting to observe that it was higher before 04.00 GMT during the post-monsoon season, with a difference of about

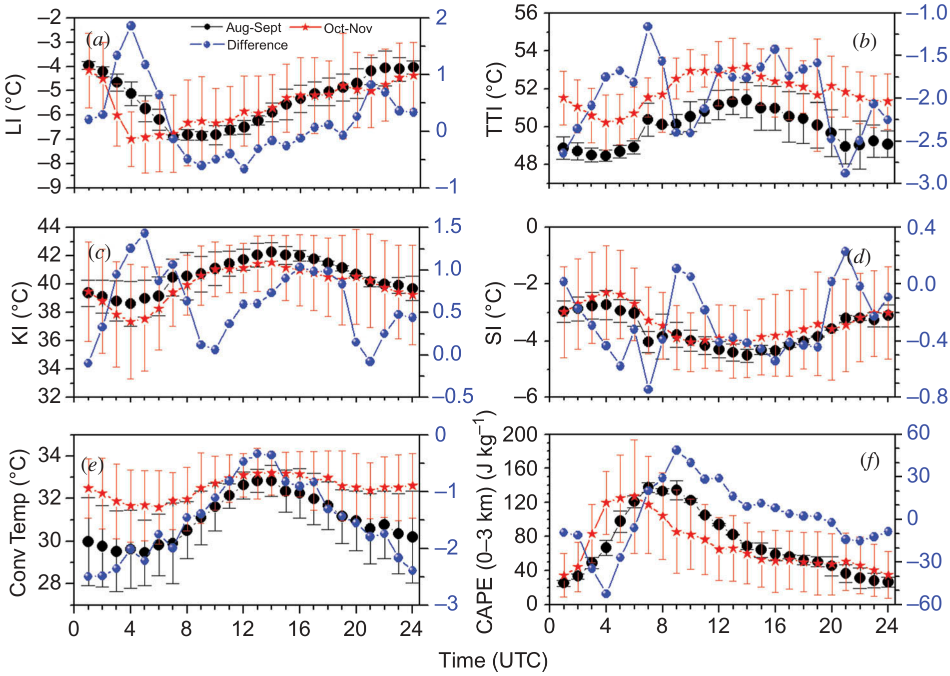


Figure 7. Seasonal variation in thermodynamic indices along with the differences between the two seasons (black: August–September; red: October–November; blue: August–September minus October–November).

60 J kg$^{-1}$. This is similar to that for LI (i.e. during the period when LI was negative, CAPE was higher). The seasonal variation suggests that thunderstorm potential is higher during the post-monsoon season (mainly early morning) over the study site.

## 5. Conclusions

In the present study, we first evaluated how well the retrieved temperature and RH profiles from MWR match with radiosonde observations. Validation of the radiometric retrieval of atmospheric temperature and humidity with radiosonde was done for the first time over this region. It is observed that the retrieved temperature (specific humidity) has a warm (wet) bias for MWR below 3 km and a cold (dry) bias above that. Also, the correlation analysis suggested that there is a bias (intercept not 0) which is height dependent (slope not 1). The RMSE calculated showed that the error in temperature (specific humidity) is less (more) below 4 km altitude. Moreover, we compared other atmospheric parameters and thermodynamic variables derived from MWR data to radiosonde observations and these were well correlated (statistically significant) with correlation greater than 0.5 for most variables. Next, considering the advantages of MWR, we utilized this for the verification of atmospheric stability over Mahbubnagar during the monsoon and post-monsoon seasons. Radiometric observations showed strong day-to-day variation in both atmospheric parameters and thermodynamic indices during the monsoon, but this was weak during the post-monsoon season. The seasonal mean of thermodynamic indices and the associated seasonal difference showed that thunderstorm potential is higher during the post-monsoon season over the study site. Our results have not only shown the variation in atmospheric stability during two different seasons, but also the robustness of ground-based microwave radiometry in meteorological applications. This is a preliminary study which needs to be verified in detail using long-term data sets.


## Acknowledgements

The authors wish to thank PDTC team members for making the CAIPEEX-IGOC campaign successful. We thank the authorities responsible for the University of Wyoming website for providing radiosonde data to the public domain. Also authors would like to thank Nelson Marta, Radiometrics Corp., for reprocessing the entire radiometer data.


## Disclosure statement

No potential conflict of interest was reported by the authors.



## References


Chan, P. W. 2009. "Performance and Application of a Multi-Wavelength, Ground-Based Microwave Radiometer in Intense Convective Weather." *Meteorologische Zeitschrift* 18: 253–265. doi:10.1127/0941-2948/2009/0375.

Chan, P. W., and K. K. Hon. 2011. "Application of Ground-Based, Multi-Channel Microwave Radiometer in the Nowcasting of Intense Convective Weather through Instability Indices of the Atmosphere." *Meteorologische Zeitschrift* 20 (4): 431–440. doi:10.1127/0941-2948/2011/0276.

Cimini, D., E. Campos, R. Ware, S. Albers, G. Giuliani, J. Oreamuno, P. Joe, S. K. Koch, S. Cober, and E. Westwater. 2011. "Thermodynamic Atmospheric Profiling During the 2010 Winter Olympics Using Ground-Based Microwave Radiometry." *IEEE Transaction on Geoscience and Remote Sensing* 40 (12): 4959–4969.

Cimini, D., T. J. Hewison, L. Martin, J. Güldner, C. Gaffard, and F. S. Marzano. 2006. "Temperature and Humidity Profile Retrievals from Ground-Based Microwave Radiometers during TUC." *Meteorologische Zeitschrift* 15 (1): 45–56. doi:10.1127/0941-2948/2006/0099.

Dai, A. 2001. "Global Precipitation and Thunderstorm Frequencies. Part II: Diurnal Variations." *Journal of Climate* 14: 1112–1128. doi:10.1175/1520-0442(2001)014<1112:GPATFP>2.0.CO;2.

Elliott, W. P., and D. J. Gaffen. 1991. "On the Utility of Radiosonde Humidity Archives for Climate Studies." *Bulletin of the American Meteorological Society* 72 (10). doi:10.1175/1520-0477(1991)072<1507:OTUORH>2.0.CO;2.

Galway, J. G. 1956. "The Lifted Index as a Predictor of Latent Instability." *Bulletin of the American Meteorological Society* 37: 528–529.

George, J. G. 1960. *Weather Forecasting for Aeronautics*, 673. New York: Academic Press.

Gettelman, A., D. J. Seidel, M. C. Wheeler, and R. J. Ross. 2002. "Multi Decadal Trends in Tropical Convective Available Potential Energy." *Journal of Geophysical Research* 107 (D21): 4606. http://dx.doi.org/10.1029/2001JD001082.

Gettelman, A., V. P. Walden, L. M. Miloshevich, W. L. Roth, and B. Halter. 2006. "Relative Humidity over Antarctica from Radiosondes, Satellites, and a General Circulation Model." *Journal of Geophysical Research* 111: D09S13. doi:10.1029/2005JD006636.

Han, Y., J. B. Snider, E. R. Westwater, S. H. Mclfi, and R. A. Ferrare 1994. "Observation of Water Vapor by Ground Based Radiometers and Raman Lidar." *Journal of Geophysical Research* 99. doi:10.1029/94JD01487.

Hewison, T., and C. Gaffard. 2003. "Radiometrics MP3000 Microwave Radiometer Performance Assessment." *Technical Report –TR29. Version 1*.

Kishore, P., M. Venkat Ratnam, S. P. Namboothiri, I. Velicogna, G. Basha, J. H. Jiang, K. Igarashi, S. V. B. Rao, and V. Sivakumar. 2011. "Global (50°S–50°N) Distribution of Water Vapor Observed by COSMIC GPS RO: Comparison with GPS Radiosonde, NCEP, Era-Interim, and

JRA-25 Reanalysis Data Sets." *Journal of Atmospheric and Solar Terrestrial Physics* 73: 1849–1860. doi:10.1016/j.jastp.2011.04.017.

Kwon, E.-H., B. J. Sohn, W. L. Smith, and J. Li. 2012. "Validating IASI Temperature and Moisture Sounding Retrievals over East Asia Using Radiosonde Observations." *Journal of Atmospheric and Oceanic Technology* 29: 1250–1262. doi:10.1175/JTECH-D-11-00078.1.

Löhnert, U., and O. Maier. 2012. "Operational Profiling of Temperature Using Ground-Based Microwave Radiometry at Payerne: Prospects and Challenges." *Atmospheric Measurement Techniques* 5: 1121–1134. doi:10.5194/amt-5-1121-2012.

Madhulatha, A., M. Rajeevan, M. Venkat Ratnam, J. Bhate, and C. V. Naidu. 2013. "Nowcasting Severe Convective Activity over Southeast India Using Ground- Based Microwave Radiometer Observations." *Journal of Geophysical Research* 118: 1–13. doi:10.1029/2012JD018174.

Miller, R. C. 1967. "Notes on Analysis and Severe Storm Fore-casting Procedures of the Military Weather Warning Center." *AWS Technical Report 200: USAF.*170 [Available from Headquarters, AWS, Scott AFB, IL 62225].

Ross, J. R., and W. P. Elliott. 1996. "Tropospheric Water Vapor Climatology and Trends over North America: 1973-93." *Journal of Climate* 9: 3561–3574.

Sanchez, J. L., R. Posada, E. Garcıa-Ortega, L. Lopez, and J. L. Marcos 2012. "A Method to Improve the Accuracy of Continuous Measuring of Vertical Profiles of Temperature and Water Vapor Density by Means of A Ground-Based Microwave Radiometer." *Atmospheric Research*, 2012.10.024. http://dx.doi.org/10.1016/j.atmosres.

Sapra, R., S. K. Dhaka, V. Panwar, R. Bhatnagar, K. Praveen Kumar, Y. Shibagaki, M. Venkat Ratnam, and M. Takahashi. 2011. "Long-Term Variations in Outgoing Long-Wave Radiation (OLR), Convective Available Potential Energy (CAPE) and Temperature in the Tropopause Region over India." *Journal of Earth System Sciences* 120 (5): 807–823. doi:10.1007/s12040-011-0113-2.

Showalter, A. K. 1953. "A Stability Index for Thunderstorm Forecasting." *Bulletin of the American Meteorological Society* 34 (6): 250–252.

Sun, B., A. Reale, D. J. Seidel, and D. C. Hunt. 2010. "Comparing Radiosonde and COSMIC Atmospheric Profile Data to Quantify Differences among Radiosonde Types and the Effects of Imperfect Collocation on Comparison Statistics." *Journal of Geophysical Research* 115: D23104. doi:10.1029/2010JD014457.

Ueno, K., and R. Aryal. 2008. "Impact of Tropical Convective Activity on Monthly Temperature Variability during Non Monsoon Season in the Nepal Himalayas." *Journal of Geophysical Research* 113: D18112. doi:10.1029/2007JD009524.

Venkat Ratnam, M., Y. Durga Santhi, M. Rajeevan, and S. Vijaya Bhaskara Rao. 2013. "Diurnal Variability of Stability Indices Observed Using Radiosonde Observations over a Tropical Station: Comparison with Microwave Radiometer Measurements." *Atmospheric Research* 124: 21–33. doi:10.1016/j.atmosres.2012.12.007.

Ware, R., R. Carpenter, J. Güldner, J. Liljegren, T. Nehrkorn, F. Solheim, and F. Vandenberghe. 2003. "A Multichannel Radiometric Profiler of Temperature Humidity and Cloud Liquid." *Radio Science* 38 (4): 8079. doi:10.1029/2002RS002856.